

PAPER • OPEN ACCESS

## An efficient structural finite element for inextensible flexible risers

To cite this article: T K Papathanasiou *et al* 2017 *IOP Conf. Ser.: Mater. Sci. Eng.* **276** 012023

View the [article online](#) for updates and enhancements.

### Related content

- [Estimating the Size and Timing of the Maximum Amplitude of Solar Cycle 24](#)  
Ke-Jun Li, Peng-Xin Gao and Tong-Wei Su
- [Comparison of equilibrium-based plasticity models and a Taylor-like hybrid formulation for deformations of constrained crystal systems](#)  
V C Prantil, P R Dawson and Y B Chastel
- [A class of nonholonomic kinematic constraints in elasticity](#)  
Joris Vankerschaver

# An efficient structural finite element for inextensible flexible risers

**T K Papathanasiou<sup>1\*</sup>, S Markolefas<sup>2</sup>, P Khazaeinejad<sup>1</sup> and H Bahai<sup>1</sup>**

<sup>1</sup>Department of Mechanical, Aerospace and Civil Engineering, Brunel University London, UK

<sup>2</sup>Department of Mechanical Engineering, Technological Educational Institute of Sterea Ellada, Chalkida, Greece

\*Contact author: theodosios.papathanasiou@brunel.ac.uk

**Abstract.** A core part of all numerical models used for flexible riser analysis is the structural component representing the main body of the riser as a slender beam. Loads acting on this structural element are self-weight, buoyant and hydrodynamic forces, internal pressure and others. A structural finite element for an inextensible riser with a point-wise enforcement of the inextensibility constraint is presented. In particular, the inextensibility constraint is applied only at the nodes of the meshed arc length parameter. Among the virtues of the proposed approach is the flexibility in the application of boundary conditions and the easy incorporation of dissipative forces. Several attributes of the proposed finite element scheme are analysed and computation times for the solution of some simplified examples are discussed. Future developments aim at the appropriate implementation of material and geometric parameters for the beam model, i.e. flexural and torsional rigidity.

## 1. Introduction and literature review

As oil exploration and production progresses into deeper waters the demand for efficient simulation and design of flexible riser systems, functioning in harsh subsea environments and operating at high internal and external pressures, increases. Numerical models used for analysis of flexible riser heavily rely on the structural component representing the main body of the riser as a slender beam [1]. This structural component is subjected to several characteristic loading conditions including self-weight, buoyant and hydrodynamic forces, and internal pressure [2]. The complexity of the geometry, deformations, material behaviour and loads acting on the riser leads to computationally intensive modelling problems. An appropriate selection of the riser structural model can significantly facilitate the analysis.

Several researchers have proposed models for flexible riser simulation and analysis. The basic component of the proposed models is a slender beam-type structural element representing the riser body. In the late 70s, Kirk et al. [3] presented a frequency domain normal mode solution for an unbuoyed riser under periodic excitation. The excitation originated from a surface vessel motion in the direction of wave propagation. Their structural analysis was based on a normal mode solution (free vibration modes and rigid body motions) of a variable tension, beam-column equation. The model utilised Morison's formula for drag forces and included the effects of a linearly varying current as



well. Subsequently, Kirk [4] employed a modal/Galerkin solution for the linearised single wave and linearised spectral frequency analysis of tension-leg-platform risers.

The importance of nonlinearities in the riser response was subsequently pointed out by several authors. Bernitsas et al. [5] presented a static, 3D, small strain-large deformation analysis of deep water risers, based on an incremental finite element predictor-corrector procedure. These authors considered both extensible and inextensible risers. Coupling of torsion and bending, as well as deformation dependent boundary conditions and external loads were included in the model. In a following study, Bernitsas and Kokarakis [6] demonstrated that differences as high as 28% in the riser maximum displacement may appear in the presence of nonlinearities. At the same time, differences of 31% in the lower ball joint angle and 40% in the maximum equivalent stress were reported by the same authors. Three dimensional nonlinear dynamic analysis has been extended to more involved configurations and applied to riser bundles by Vlahopoulos and Bernitsas [7]

A different modelling approach, based on the lumped mass discretisation method was presented by Ghadimi [8]. A time domain solution using tangent stiffness increments and Wilson-theta numerical integration was utilised by this author. The proposed analysis featured also a simple seabed contact model for catenary risers. The simulation strategy was reported to produce results in good agreement with experiments. Trim [9] retained the small displacement structural model using finite elements and the modal form but supplemented it with nonlinearities originating from the fluid forcing and stochastic attributes of some parameters.

Regarding analytical or semi-analytical techniques, Cheng et al. [10] analysed linear vibrations of marine risers using perturbation techniques to derive asymptotic expansions based on the dynamic stiffness methods. In their analysis they employed and extended previous results reported by Kim and Triantafyllou [11]. A very simple model, admitting analytic solution, for the axial dynamic response of marine risers in installation was proposed by Wang et al. [12]. The same authors used also the finite difference method to analyse statically the combined effect of axial and lateral forces of marine risers [13].

More recent advances in the analysis and simulation of flexible risers include several studies focusing on complex dynamic analysis or the analysis of structural behaviour. Rahmati, Norouzi et al. [14] experimentally and numerically analysed the behaviour of flexible risers under bending, taking into account the internal structure of the component. Klaycham et al. [15] employed the finite element method to analyse the nonlinear vibrations of marine risers accounting for large displacements and taking into account the strain energy associated with the rotational restraint at the bottom end of the riser. Zhu et al. [16] studied that possibility of energy harvesting using a flexible riser and attached free-to rotate impellers. Finally, Cuamatzi-Melendez et al. [17] discussed the bisymmetric collapses in flexible risers in high external pressure environments.

The above literature review is not exhaustive, but rather indicative of the developments in the analysis and simulation of flexible risers within the last decades. Of major importance is the observation that the structural component representing the flexible riser is typically considered to have nonlinear response and very complex dynamics, while at the same time simplicity in the formulation of the governing equations and efficiency in the solution are desired.

In this study, a structural finite element for an inextensible riser, based on the approach developed in [1] regarding the application of the inextensibility constraint, is presented. In particular, the inextensibility constraint is applied only at the nodes of the meshed arc length parameter. Among the virtues of the proposed approach is the flexibility in the application of boundary conditions and the easy incorporation of dissipative forces. Several attributes of the proposed finite element scheme are analysed and CPU times for the solution of many simplified examples are computed. Future developments aim at the appropriate implementation of material and geometric parameters for the inextensible beam model, i.e. flexural and torsional rigidity. These data will be generated by the multi-scale model for flexible riser systems developed in [2].

## 2. Organisation of paper

The paper is organised as follows: in Section 3 the governing equations for an inextensible beam featuring a nonlinear bending moment-curvature relation are derived from the variation of the energy functional. Based on the variational form of the problem a finite element procedure, similarly to the one proposed in [1] is presented in Section 4. The main result, i.e. the formulation of a numerical scheme that features a linearization of the nonlinear flexural modulus and preserves the convergence rate characterising the method of Bartels [1] is contained in this section. Finally, Section 5 is devoted to the presentation of relevant numerical results. The study ends with a concluding paragraph summarising the current findings and mentioning future developments. In particular, the proposed scheme refers to the flexural response of the beam and does not include the effects of torsion. This addition, is very important and is targeted as a near future step towards the development of an integrated methodology for the efficient and robust simulation of flexible risers.

## 3. Governing equations

In this section, the equation governing the large deflection of inextensible beams will be introduced and briefly analysed. Subsequently, the finite element procedure introduced by Bartels [1] is adopted for the simulation of elements representing flexible riser components. The analysis presented here is focused on the riser body itself and does not incorporate fluid-structure interaction phenomena. The aim is to first obtain an efficient model, and an associated robust solution methodology for the inextensible structural member undergoing large deformations and featuring some degree of nonlinearity in the moment-curvature constitutive relation.

Let  $L$  and  $T$  be positive constants representing the length of inextensible beam and the total time that the phenomenon under consideration lasts, respectively. The beam domain is  $I = [0, L]$ . For any  $s \in I$ , the vector valued function

$$u(s) = [x(s) \quad y(s) \quad z(s)]^T, \quad (1)$$

defines the location in the Euclidian space of each point along the length of the inextensible beam. The curvature at each point  $s$  representing the arc-length parameter is  $\kappa(s) = u_{ss}$ , where a subscript denotes differentiation with respect to the respective variable.

The kinetic energy of a flexible riser with variable properties is

$$K(\partial_t u) = \frac{1}{2} \int_I m |\partial_t u|^2 ds, \quad (2)$$

where  $m$  is the mass distribution along the riser body and  $|\partial_t u|$  denotes the measure of the velocity vector. In the following analysis, the strain energy functional is assumed to have the form

$$U(u) = \frac{1}{2} \int_I EI |u_{ss}|^2 ds + \frac{1}{4} \int_I b |u_{ss}|^4 ds, \quad (3)$$

where  $EI = EI(s)$  represents the flexural rigidity of the riser and  $b = b(s)$  is a parameter introducing nonlinear elastic behaviour in the response. This expression of the strain energy is aimed to simulate phenomena related to relatively small values of the curvature, by introducing a small degree of nonlinearity to the moment-curvature relation.

Assuming now an energy functional of the form

$$J(\partial_t u, u, \lambda) = K(\partial_t u) + U(u) + \frac{\lambda}{2} \int_I (|u_s|^2 - 1) ds, \quad (4)$$

in order to incorporate the inextensibility constraint through a Lagrange multiplier  $\lambda$  representing the action that enforces the inextensibility and setting the first variation, using the Gâteaux derivative, to be zero, it is

$$\lim_{\varepsilon \rightarrow 0} = \frac{J(\partial_t u + \varepsilon \partial_t \chi, u + \varepsilon \chi, \lambda + \varepsilon \mu) - J(\partial_t u, u, \lambda)}{\varepsilon} = 0. \quad (5)$$

Equation (5) implies the variational form:

$$\int_I m \partial_{tt} u \cdot \chi ds + \int_I (EI + b |u_{ss}|^2) u_{ss} \cdot \chi_{ss} ds + \int_I \lambda u_s \cdot \chi_s ds = 0, \tag{6}$$

and

$$|u_s|^2 - 1 = 0 \text{ in } I, \tag{7}$$

almost everywhere in  $(0, T)$  for all admissible functions  $\chi$ .

Introducing now the nondimensional quantities  $\tilde{s} = s / L$ ,  $\tilde{u} = u / L$  and  $\tilde{t} = t L^{-2} \sqrt{EI / m}$ , the variational form becomes (after dropping tildes)

$$\int_I \partial_{tt} u \cdot \chi ds + \int_I (1 + B |u_{ss}|^2) u_{ss} \cdot \chi_{ss} ds + \int_I \Lambda u_s \cdot \chi_s ds = \int_I Q \cdot \chi ds, \tag{8}$$

where  $B = bL^{-2} / EI$ ,  $\Lambda = \lambda L^3 / EI$  and  $Q = qL^3 / EI$  and  $I = [0, 1]$ .

In the nondimensional form, the strain energy density as a function of the curvature  $\kappa = u_{ss}$  reads

$$V(\kappa) = \frac{1}{2} |\kappa|^2 + \frac{1}{4} b |\kappa|^4. \tag{9}$$

A plot of the  $V$  as a function of  $\kappa$ , for different values of the nonlinearity parameter  $b$  is depicted in Figure 1. The bending moment for the above model, defined as the energy conjugate quantity of the curvature is

$$M(\kappa) = (1 + B |\kappa|^2) \kappa. \tag{10}$$

A plot of the bending moment as a function of the curvature is depicted in Figure 2 for different values of the nonlinearity parameter  $B$ . Finally, a plot of the bending modulus, denoted here as  $dM/d\kappa$  is shown in Figure 3. The feasible domains for the above mentioned quantities are highlighted in green color. For  $B = 0$  the linear bending moment-curvature model is retrieved. Positive values of  $B$  correspond to a type of elastic hardening in the behaviour of the beam, while negative values produce a reduction in the flexural rigidity, with increasing curvature.

This particular model can be employed up to values of curvature that retain the positive definiteness of the strain energy in order to simulate the small curvature region of the more involved behaviour that has been proposed in [2].

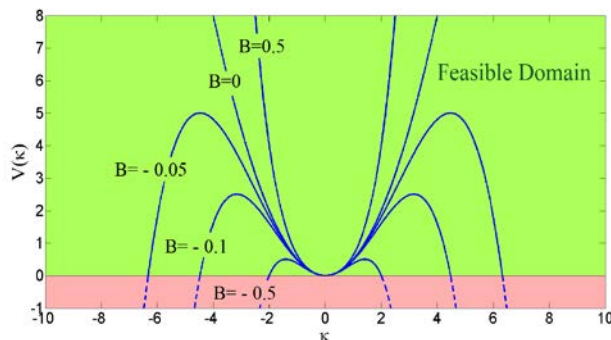


**Figure 1.** Strain energy density for different values of the nonlinearity parameter  $B$ .

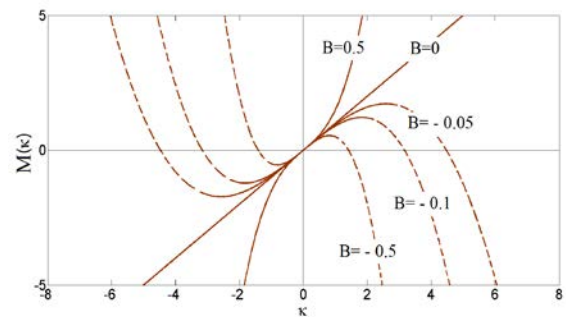


**Figure 2.** Bending moment for different values of the nonlinearity parameter  $B$ .

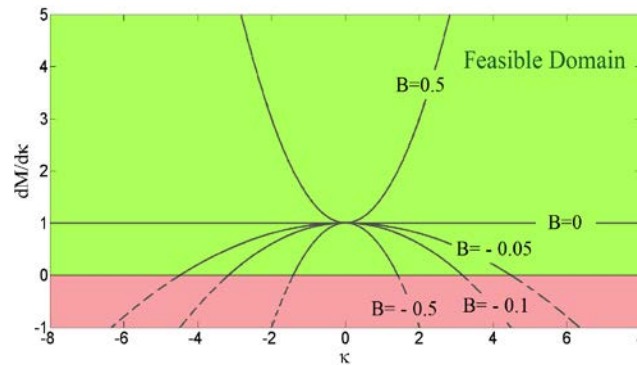


**Figure 3.** Flexural rigidity for different values of the nonlinearity parameter  $B$ .

#### 4. The proposed finite element scheme

For the efficient solution of the inextensible beam model equations presented in the previous section, the numerical procedure proposed by Bartels [1] for the vibration of inextensible curves of constant flexural rigidity is utilised. The efficient method proposed by Bartels, based on the satisfaction of the inextensibility constraint only on the nodes of the finite element mesh, is extended here to the case of an inextensible beam that has a curvature dependent flexural modulus and in particular a bending moment-curvature relation as defined in Equation (10). It should be noted that the scheme proposed here includes only the flexural response of the riser and for realistic applications it should be coupled with axial and torsional effects as well. In the following, basic steps for the derivation of an integrated methodology for the efficient and robust simulation of flexible risers are described. Initially, following Bartels [1], for the time discretisation of the system the backward difference quotient  $D^-$  is introduced in Equation (11)

$$D^- v^{n+1} = \frac{v^{n+1} - v^n}{\tau}, \quad (11)$$

In the above expression  $v^n$  denotes the velocity of the system  $\partial_t u$  at time instant  $t_n$  and  $\tau = t_{n+1} - t_n$  is the time step (assumed constant in this study but in general variable). Furthermore, the update (12) of the deflection is introduced:

$$u^{n+1} = u^n + \tau v^{n+1}, \quad (12)$$

The scheme involving spatial discretisation using standard Hermite interpolation for each finite element and expressions Equation (11) and Equation (12) for discretisation with respect to time is:

Given  $u^j, v^j \in H^2(I; \mathbb{R}^3)$ ,  $j = 0, 1, 2, \dots, n$  and  $\tau > 0$ , find  $v^{k+1} \in H^2(I; \mathbb{R}^3)$  such that

$$\int_I D^- v^{n+1} \cdot \chi ds + \int_I \left( 1 + B |u_{ss}^n + \tau v_{ss}^{n+1}|^2 \right) [u_{ss}^n + \tau v_{ss}^{n+1}] \cdot \chi_{ss} ds = 0, \quad (13)$$

and  $v_s^{n+1} \cdot u_s^n = 0$  in  $I$ , for all  $\chi \in H^2(I; \mathbb{R}^3)$ , with  $\chi_s \cdot u_s^n = 0$  in  $I$ . Update the deflection through  $u^{n+1} = u^n + \tau v^{n+1}$ , where  $H^2(I; \mathbb{R}^3)$  denotes the space of functions with square-integrable second derivatives defined in  $I$ , with values in the Euclidian space  $\mathbb{R}^3$ . The value  $j = 0$  corresponds to the definition of appropriate initial conditions for the deflection and velocity of the inextensible beam.

For the approximate solution of the above problem, using the definition of  $D^- v^{n+1}$ , multiplying the discrete variational form by  $\tau$  and expanding the terms in the second integral we obtain

$$\begin{aligned}
& (v^{n+1} - v^n, \chi) + \tau \left( \left[ 1 + B |u_{ss}^n|^2 \right] u_{ss}^n, \chi_{ss} \right) \\
& + \tau^2 \left( \left[ 1 + B |u_{ss}^n|^2 \right] v_{ss}^{n+1}, \chi_{ss} \right) + 2\tau^2 \left( B [u_{ss}^n \cdot v_{ss}^{n+1}] u_{ss}^n, \chi_{ss} \right) \\
& + \tau^3 \left( B |v_{ss}^{n+1}|^2 u_{ss}^n, \chi_{ss} \right) + 2\tau^3 \left( B [u_{ss}^n \cdot v_{ss}^{n+1}] v_{ss}^{n+1}, \chi_{ss} \right) \\
& + \tau^4 \left( B |v_{ss}^{n+1}|^2 v_{ss}^{n+1}, \chi_{ss} \right) = 0
\end{aligned} \tag{14}$$

where  $(\cdot, \cdot)$  denotes the  $L^2(I)$  inner product defined by the integrals in the definition of the discrete problem. Using now the identity

$$\left( u_{ss}^n \cdot v_{ss}^{n+1} \right) u_{ss}^n = \left( u_{ss}^n \otimes u_{ss}^n \right) v_{ss}^{n+1}, \tag{15}$$

the following result is easily derived from Equation (14).

**PROPOSITION** Let  $\mathbf{I}_3$  denote the  $3 \times 3$  identity matrix. Then it is

$$\begin{aligned}
& (v^{n+1}, \chi) + \tau^2 \left( \left[ \mathbf{I}_3 + B |u_{ss}^n|^2 \mathbf{I}_3 + 2B (u_{ss}^n \otimes u_{ss}^n) \right] v_{ss}^{n+1}, \chi_{ss} \right) = \\
& (v^n, \chi) - \tau \left( \left[ 1 + B |u_{ss}^n|^2 \right] u_{ss}^n, \chi_{ss} \right) + O(\tau^3)
\end{aligned} \tag{16}$$

The above proposition suggests that the simpler form Equation (16) can be used instead of Equation (14), while the remainder is of the order  $O(\tau^3)$ . This is a higher order term compared to the order of approximation in the finite element procedure employed by Bartels [1] and thus the use of Equation (16) instead of Equation (14) does not affect the rate of convergence.

The linearized updated procedure defined by Equation (16) has certain similarities with the *secant modulus* method (method of Kačanov), however it is not identical with the secant modulus method obtained by linearizing the problem and then introducing the backward difference quotient for the time derivative approximation. For the approximation of the displacement field either 2- node Hermite elements or 3-node Hermite elements [18] can be used.

## 5. Numerical results and discussion

In this section, the efficiency of the proposed model and the numerical solution strategy is investigated. The possible use of the proposed finite element for applications involving the large deflection of flexible marine risers (Figure 4), featuring large displacements in the 3D space, various types of boundary conditions and possible large masses with degrees of freedom attached at one end (representing possibly a vessel motion due to surface gravity wave fields) is discussed.

Regarding the effectiveness of the proposed methodology and the effect of the nonlinearity in the moment-curvature relation, one of the examples studied in [1] will be analysed for different values of the nonlinearity parameter  $B$ . In particular, the case of an unwinding helix is selected. Following Bartels [1], we select  $I = [0, 2\pi]$ ,  $T = 30$  and

$$u(s, 0) = \left[ \sin(\sqrt{0.99}s) \quad \cos(\sqrt{0.99}s) \quad \sqrt{0.01}s \right], \quad v(s, 0) = [0 \quad 0 \quad 0],$$

while at  $s = 0$  it is

$$u(0, t) = [0 \quad 1 \quad 0], \quad u_s(0, t) = \left[ \sqrt{0.99} \quad 0 \quad \sqrt{0.01} \right],$$

representing clamped boundary conditions.

Figures 5 and 6 present snapshots of the unwinding helix evolution for the linear bending moment-curvature model (blue line) and the nonlinear case (red line).

In Figure 5, the case  $B = -0.025$  is examined, corresponding to a ‘softening’ flexural modulus with increasing curvature, while in Figure 6, it is  $B = 0.1$  (red line), corresponding to a flexural modulus that increases with increasing values of the curvature measure. The results for  $B = 0$  are also included. This case is presented for two reasons. First, it provides a means of validation since it has already been analysed in [1]. The results obtained in this study for  $B = 0$  are identical to those obtained by Bartels [1]. The second reason is to demonstrate the effect that the nonlinearity in the bending behaviour of the beam has on the deflections. To that end, the linear case is retained as a reference.

The violation of the inextensibility constraint (that is the total increase in the length of the beam) in the examples presented in Figures 5 and 6 is at the most 0.05 in a total (nondimensional) length of 6.28. As reported also in [1], if the time increment is appropriately selected for a given spatial mesh size, the present numerical scheme should approximate the inextensibility feature very effectively. The time needed for the solution of the above presented examples is only a few minutes. The number of 2-node elements used is 30 and the time steps less than 2000.

As a second example, a helix with two concentrated masses attached at its ends is studied. The mass at the lower end is assigned a very large value, leading to virtually zero motion of the lower end. This case would approximately correspond to a fixed end. Such an edge condition would be appropriate for the simulation of the riser connection to the seabed. The mass attached at the upper end is significantly lower and thus the upper end undergoes significant displacements. This type of edge condition might be relevant to the attachment of a flexible riser onto a vessel or a floating platform. In the nondimensional setting, the mass attached to the lower end is  $10^6$ , while the one at the upper end is 100. The remaining parameters are  $I = [0, 4\pi]$ ,  $T = 30$  and

$$u(s, 0) = [\sin(\sqrt{0.25}s) \quad \cos(\sqrt{0.25}s) \quad \sqrt{0.75}s], \quad v(s, 0) = [0 \quad 0 \quad 0],$$

while at  $s = 0$  it is

$$u(0, t) = [0 \quad 1 \quad 0], \quad u_s(0, t) = [\sqrt{0.27} \quad 0 \quad \sqrt{0.75}].$$

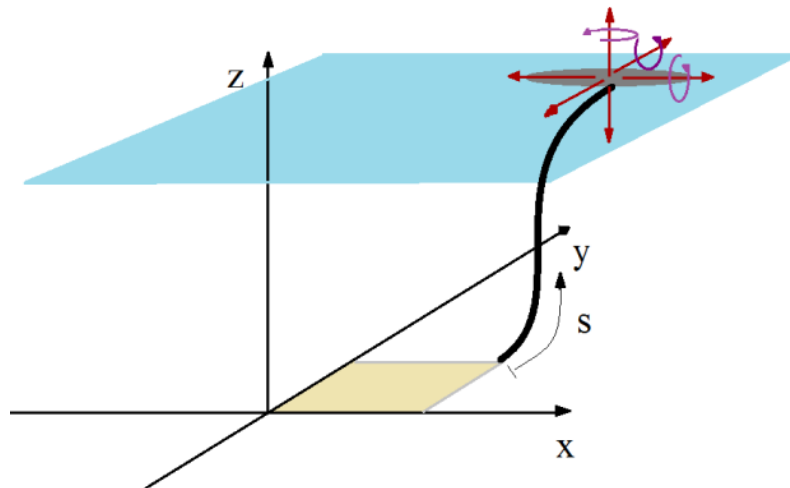


**Figure 4.** Schematic representation of a flexible marine riser.

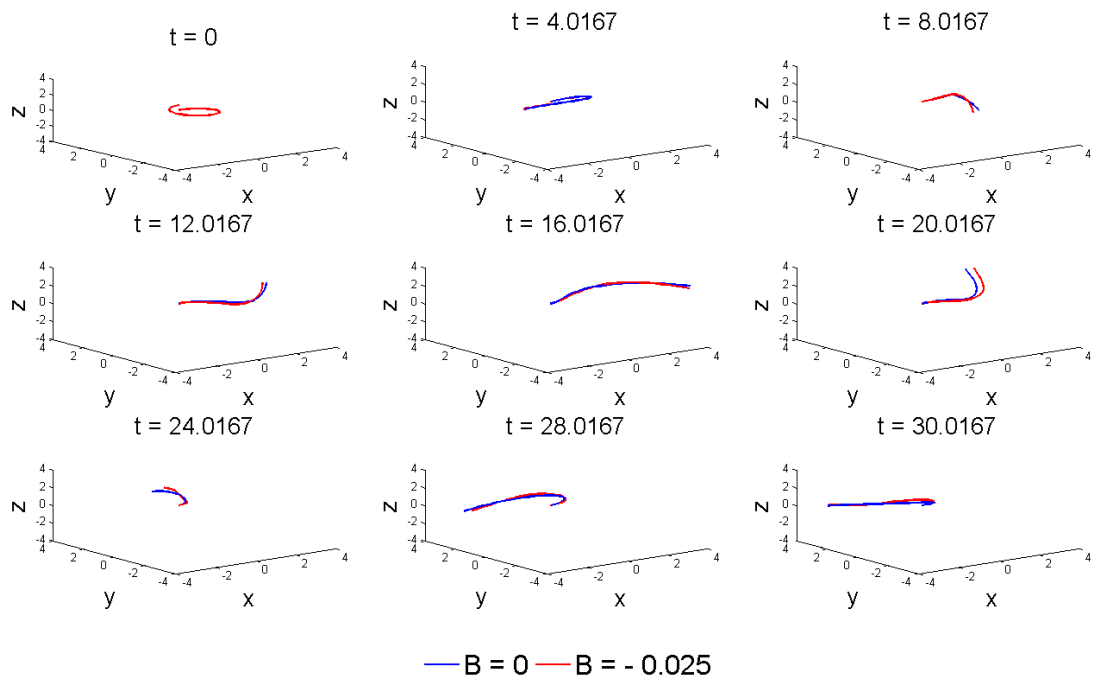


**Figure 5.** Evolution of the unwinding helix for  $B = 0$  and  $B = -0.025$ .

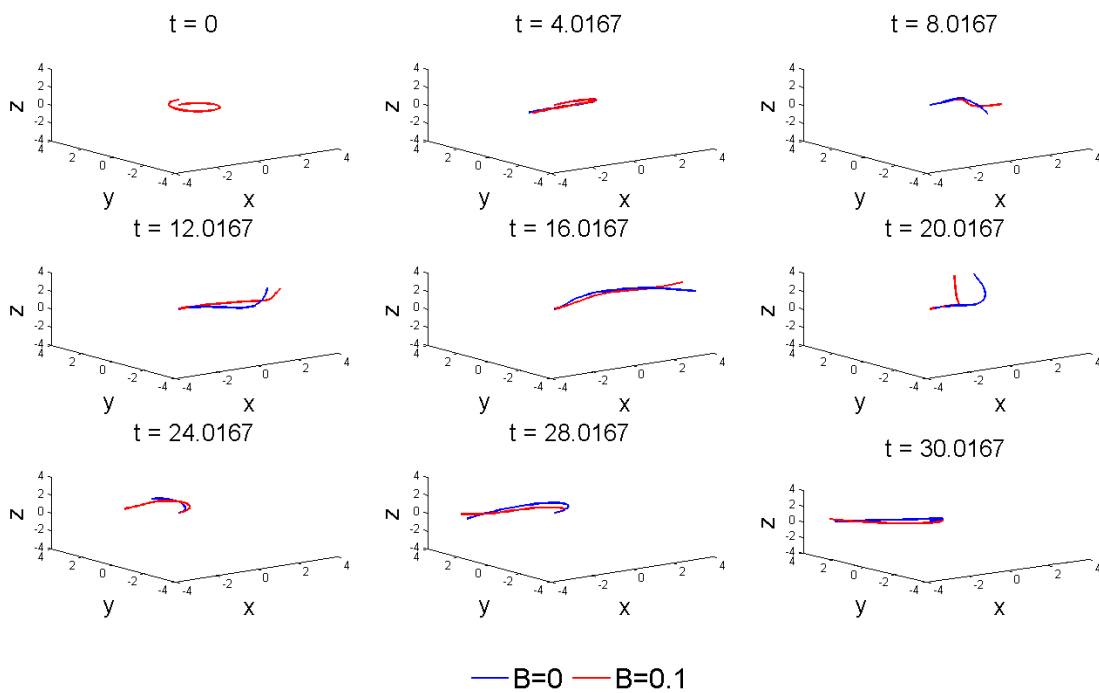


**Figure 6.** Evolution of the unwinding helix for  $B = 0$  and  $B = 0.1$ .

Again the violation in the inextensibility constraint leads to an insignificant variation in the total length of the beam, even in cases where very few elements and time steps are used. In all the examined cases, the total time needed for the evaluation of the evolution was only a few minutes. This suggests that the efficient solution methodology proposed in [1], and applied to the case of riser like structures in the present work, might be of significant interest when multiple simulations for the purpose of parametric studies are needed. Snapshots of the evolution in the beam deflection are depicted in Figure 7. The velocity along the length of the beam is also depicted in the form of arrows. It should be noted that the selected example corresponds to the case  $B = 0$ .

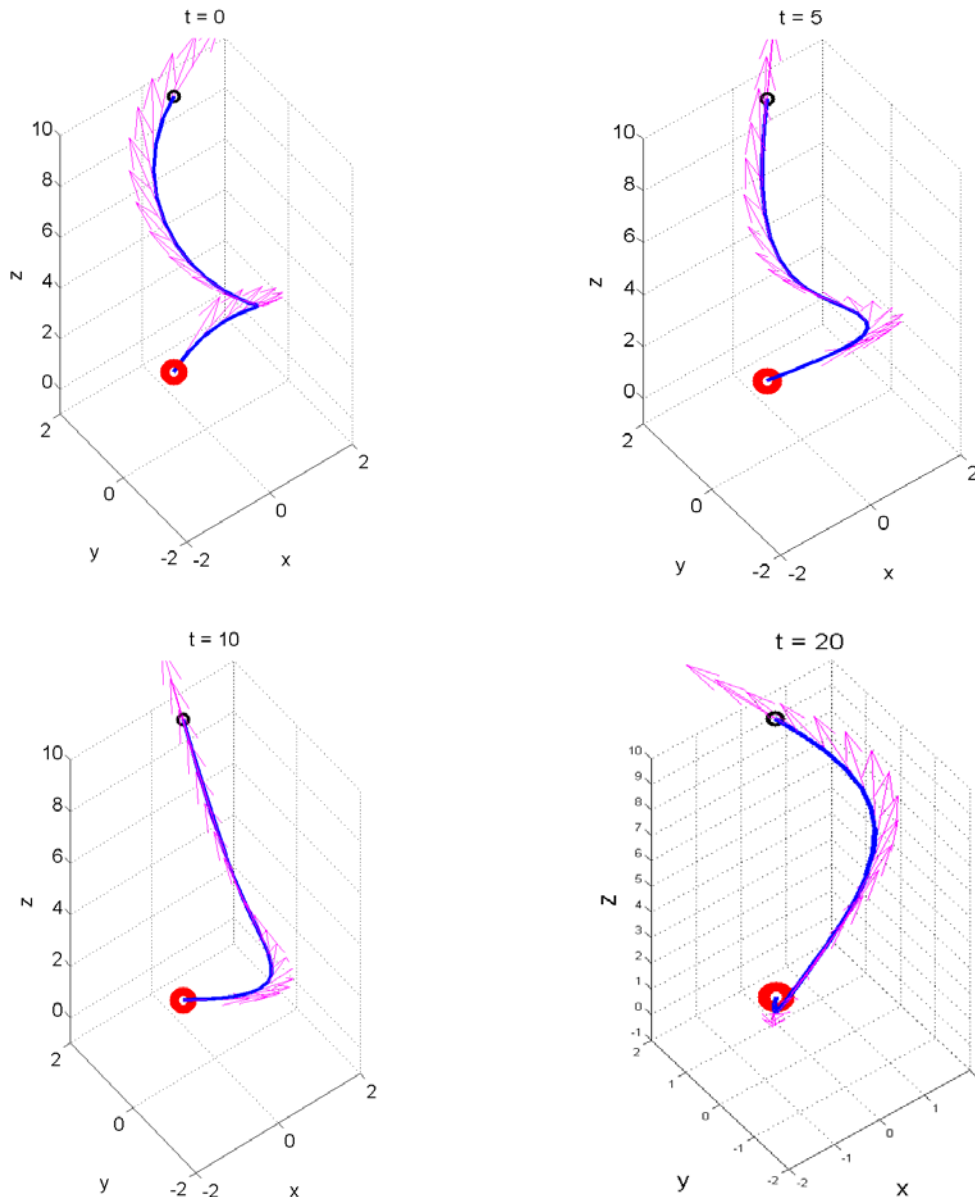


**Figure 7.** Snapshots of the evolution (example 2) for  $B = 0$ .

## 6. Conclusions

In this study, a structural finite element for an inextensible riser, based on a point-wise application of the inextensibility constraint is presented. In particular, the inextensibility constraint is applied only at the nodes of the meshed arc length parameter. The method is extended to include some degree of

nonlinearity in the curvature-bending moment relation. The specific form adopted corresponds to the small curvature regime of more sophisticated riser mechanical behaviour models proposed in the literature. Future research focuses on the incorporation of the torsion effects while retaining the robustness of the numerical solution technique developed. Among the virtues of the proposed approach is the flexibility in the application of boundary conditions and the easy incorporation of dissipative forces.

## References

- [1] Bartels S 2016 A simple scheme for the approximation of elastic vibrations of inextensible curves *IMA J. Numer. Anal.* **36** pp 1051-71.
- [2] Rahmati M T, Bahai H and Alfano G 2016 An accurate and computationally efficient small-scale nonlinear FEA of flexible risers *Ocean Eng.* **121** pp. 382-91.
- [3] Kirk C L, Etok E U and Cooper M T 1979 Dynamic and static analysis of a marine riser *Appl. Ocean Res.* **1** pp 125-35.
- [4] Kirk C L 1985 Dynamic response of marine risers by single wave and spectral analysis methods *Appl. Ocean Res.* **7** pp 2-13.
- [5] Bernitsas M M, Kokarakis J E and Imron A. 1985 Large deformation three-dimensional static analysis of deep water marine risers *Appl. Ocean Res.* **7** pp. 178-87.
- [6] Bernitsas M M and Kokarakis J E 1988 Importance of nonlinearities in static riser analysis *Appl. Ocean Res.* **10** pp 2-9.
- [7] Vlahopoulos N and Bernitsas M.M. 1991 Three-dimensional nonlinear dynamics of nonintegral riser bundle *J. Ship Res.* **35** pp. 40-57.
- [8] Ghadimi R. 1988 A simple and efficient algorithm for the static and dynamic analysis of flexible marine risers *Comput. Struct.* **29** pp. 541-55.
- [9] Trim A D 1990 Time-domain random dynamic analysis of marine risers and estimation of non-Gaussian bending stress statistics *Appl. Ocean Res.* **12** pp. 162-74.
- [10] Cheng Y, Kim Vandiver J. and Moe G. 2002 The linear vibration analysis of marine risers using the WKB-based dynamic stiffness method *J. Sound Vib.* **251** pp. 750-60.
- [11] Kim Y C and Triantafyllou M S 1984 The nonlinear dynamics of long slender cylinders *J. Energy Resour. Technol.* **106** pp 250-56.
- [12] Wang Y, Gao D and Fang J 2014 Axial dynamic analysis of marine riser installation *J. Nat. Gas Sci. Eng.* **21** pp. 112-17.
- [13] Wang Y, Gao D and Fang J 2014 Static analysis of deep-water marine riser subjected to both axial and lateral forces in its installation *J. Nat. Gas Sci. Eng.* **19** pp 84-90.
- [14] Rahmati M T, Norouzi S, Bahai H and Alfano G 2017 Experimental and numerical study of structural behaviour of a flexible riser model *Appl. Ocean Res.* **67** pp 162-168.
- [15] Klaycham K, Athisakul C and Chucheepsakul S 2017 Nonlinear vibration of marine riser with large displacement *J. Marine Sci. Technol.* **22** pp. 361-75.
- [16] Zhu H and Gao Y 2017 Vortex induced vibration response and energy harvesting of a marine riser attached by a free to rotate impeller *Energy* **134** pp 532-44.
- [17] Cuamatzip-Melendez R, Castillo-Hernandez O, Vazquez-Hernandez A O and Vaz M A 2017 Finite element and theoretical analyses of bisymmetric collapses in flexible risers for deepwaters developments *Ocean Eng.* **140** pp 195-208.
- [18] Papatthaniou T K, Karperaki A, Theotokoglou E E and Belibassakis K A 2014 A higher order FEM for time-domain hydroelastic analysis of large floating bodies in an inhomogeneous shallow water environment *Proc. Royal Soc. A* 471 20140643.
- [19] Ong M C, Bachynski E E and Økland O D 2017 Dynamic Responses of Jacket-Type Offshore Wind Turbine Using Decoupled and Coupled Models *J. Offshore Mech. Arct. Eng.* **139** 041901.